JOURNAL OF BACTERIOLOGY, May 1997, p. 3021–3029 Vol. 179, No. 9
0021-9193/97/$04.00+0

Identification and Characterization of *pbpA* Encoding *Bacillus subtilis* Penicillin-Binding Protein 2A

THOMAS MURRAY, DAVID L. POPHAM,† AND PETER SETLOW*

Department of Biochemistry, University of Connecticut Health Center, Farmington, Connecticut 06030

Received 23 December 1996/Accepted 13 February 1997

Amino acid sequence analysis of tryptic peptides derived from purified penicillin-binding protein PBP2a of *Bacillus subtilis* identified the coding gene (now termed *pbpA*) as *yqgF*, which had been sequenced as part of the *B. subtilis* genome project; *pbpA* encodes a 716-residue protein with sequence similarity to class B high-molecular-weight PBPs. Use of a *pbpA-lacZ* fusion showed that *pbpA* was expressed predominantly during vegetative growth, and the transcription start site was mapped using primer extension analysis. Insertional mutagenesis of *pbpA* resulted in no changes in the growth rate or morphology of vegetative cells, in the ability to produce heat-resistant spores, or in the ability to trigger spore germination when compared to the wild type. However, *pbpA* spores were unable to efficiently elongate into cylindrical cells and were delayed significantly in spore outgrowth. This provides evidence that PBP2a is involved in the synthesis of peptidoglycan associated with cell wall elongation in *B. subtilis*.

Penicillin-binding proteins (PBPs) are enzymes involved in a number of reactions of peptidoglycan biosynthesis and have been divided into three classes based on sequence similarity (9). In *Escherichia coli*, the class A high-molecular-weight PBPs have been shown to possess a transglycosylase activity involved in polymerization of the peptidoglycan's sugar backbone (13, 18, 37). The class A and class B high-molecular-weight PBPs of *E. coli* exhibit transpeptidase activity, which results in peptide cross-links between adjacent glycan strands (11–13, 18, 37), while the low-molecular-weight PBPs of *E. coli* and *Bacillus subtilis* are most often carboxypeptidases (9, 15, 38).

In *B. subtilis* PBPs are involved not only in the synthesis of the peptidoglycan sacculus but also in the synthesis of both the germ cell wall and the cortex of the dormant spore. The latter structure is different from the vegetative cell wall peptidoglycan in that the spore cortex contains muramic acid lactam residues (39). Alteration of the spore cortex structure can affect spore resistance properties as well as spore germination and outgrowth (3, 10, 23–25).

To understand in detail the contribution of individual PBPs to cell and spore properties as well as to peptidoglycan structure in *B. subtilis*, we have been identifying and characterizing the genes encoding these proteins (17, 26–29). With the exception of PBP2b, which is an essential protein (41), the loss of individual PBPs in *B. subtilis* has not been associated with dramatic phenotypic changes (17, 26–29, 40). Indeed, cells lacking as many as three class A high-molecular-weight PBPs (PBP1, PBP2c, and PBP4) are viable, exhibiting only a slight growth defect, indicating a redundancy of function amongst the different high-molecular-weight PBPs (30). Furthermore, while PBP2b is thought to be responsible for septum formation in *B. subtilis* (41), no single *B. subtilis* PBP responsible for cell elongation has been identified. In contrast, mutations in *pbpA* encoding PBP2 of *E. coli* result in the production of spherical cells, indicating a preeminent role for PBP2 in maintenance of the rod-like shape of the cell (35).

To date the only major PBP of *B. subtilis* whose coding gene has not been identified is PBP2a. This PBP was initially identified as component II when PBPs were first described in *B. subtilis* by Blumberg and Strominger (4) and was later called PBP2a after the discovery of PBP2b (14). In this work we identify the gene encoding this protein, characterize its expression, and demonstrate that while the loss of PBP2a is not associated with phenotypic changes during vegetative growth, mutant spores are unable to efficiently make the transition from a germinated spore to a cylindrical cell during outgrowth. The evidence presented here predicts that the major role for PBP2a in *B. subtilis* is in cell elongation during germination and outgrowth.

MATERIALS AND METHODS

Bacterial strains and growth conditions. The *B. subtilis* strains used are derived from 168 and are listed in Table 1. *B. subtilis* was grown and sporulated at 37°C in 2× SG medium (16). Spores were purified by repeated washes with H_2O and then stored in H_2O at 4°C as previously described (20). Bacterial spores were heat shocked in H_2O for 30 min at 70°C prior to germination in 2× YT medium (16 g of tryptone, 10 g of yeast extract, and 4 g of NaCl, per liter of H_2O) with 4 mM L-alanine as described previously (25). Spore heat resistance was measured as described previously (25) by heating the spores in water at 85°C for 15 min. *B. subtilis* was transformed to chloramphenicol resistance (Cm^r; 3 μg/ml) as described previously (1). *E. coli* was grown in 2× YT medium with ampicillin (50 μg/ml) at 37°C.

Peptide sequencing, enzyme assays, and membrane and spore cortex preparation. Strain PS1900, which lacks the abundant PBP5, was grown to an optical density of around 3.0 in 10 liters of 2× YT medium. Cells were harvested, and total PBPs were isolated via penicillin affinity chromatography as previously described (26). Individual PBPs were separated by sodium dodecyl sulfate (SDS)-polyacrylamide gel electrophoresis (PAGE), transferred to a polyvinylidene difluoride membrane, and stained with 0.1% amido black as described previously (17, 21). The PBP2a band was cut out and digested with trypsin; tryptic peptides isolated by high-pressure liquid chromatography (HPLC) were sequenced as described previously (21). The isolation of *B. subtilis* membranes from vegetative cells growing in 2× SG medium at 37°C, labeling of PBPs with fluorescein–hexanoic-6-amino-penicillanic acid (FLU-C_6-APA) and their separation using SDS-PAGE was as described previously (30). The spore cortex was purified essentially as previously described (3) and analyzed by reverse-phase HPLC after digestion with mutanolysin (Sigma) (3, 23). β-Galactosidase assays using the substrate *o*-nitrophenyl-β-D-galactopyranoside with lysozyme extracts of vegetative cells, germinated spores, and decoated dormant spores were as previously described (20, 27).

* Corresponding author. Phone: (860) 679-2607. Fax: (860) 679-3408. E-mail: setlow@sun.uchc.edu.

† Present address: Department of Biology, Virginia Polytechnic Institute and State University, Blacksburg, VA, 24061-0406.

TABLE 1. *B. subtilis* strains and plasmids used

B. subtilis strain or plasmid	Genotype and/or construction	Source or reference
Strains		
PS832	Wild type, trp$^+$ revertant of 168	Stock
JT185	*dacA*::Cm^r	38
PS1900	*dacA*::Cm^r, JT185→PS832[a]	25
PS2462	*pbpA-lacZ* at *pbpA*, pTMA2 → PS832	This work
PS2463	*pbpA-lacZ* at *amyE*, pTMA3 → PS832	This work
PS2465	*pbpA*::pTMA4 Cm^r, pTMA4 → PS832	This work
Plasmids		
pTMA1	Upstream and N-terminal coding region of *pbpA* in pUC19	
pTMA2	Upstream and N-terminal coding region of *pbpA* fused to *lacZ* in pJF751a	
pTMA3	Upstream and N-terminal coding region of *pbpA* fused to *lacZ* in pDG268	
pTMA4	Fragment internal to the *pbpA* coding sequence in pJH101	

[a] →, transformation of chromosomal or plasmid DNA.

PCR amplification of *pbpA* and upstream regions. Two primers were used to amplify by PCR a 602-bp fragment containing the first 306 bp of *pbpA* and 296 upstream bp. PBPA1 (30-mer, 5′GGCCCTTCTGAAAGAGGATGTGGGAATTCC3′, nucleotides (nt) 135363 to 135392 in DDBJ D84432) was designed to take advantage of an *Eco*RI site present in the sequence (underlined) to aid in cloning. PBPA2 (34-mer, 3′-GATTTAGCTGGTGCGTTCTTGTCGCGCCTAGGCG5′, complementary to nt 135965 to 135990 in DDBJ D84432) contained an added 5′ *Bam*HI site and flanking residues (underlined) to assist in cloning. The resulting *Eco*RI-*Bam*HI fragment was cloned into pUC19, generating plasmid pTMA1; the insert in this plasmid was sequenced using an automated DNA sequencer (373 DNA Sequence System; Applied Biosystems) to confirm that the PCR product had the correct sequence. The *Eco*RI-*Bam*HI fragment was cut out of pTMA1 and cloned into pJF751a (36) and pDG268 (2) in *E. coli* JM83 by standard methods, generating plasmids pTMA2 and pTMA3, respectively (Fig. 1). pTMA2 and pTMA3 were used to transform *B. subtilis* to Cm^r, generating transcriptional *pbpA-lacZ* fusions at the *pbpA* locus (strain PS2462) and the *amyE* locus (strain PS2463); both of these constructs retained a wild-type copy of *pbpA*. Finally, a 232-bp *Ssp*I-*Bam*HI fragment (note that the *Bam*HI site was introduced by PCR) within the *pbpA* coding sequence was cloned into pJH101 (8). The resulting plasmid, pTMA4 (Fig. 1), was used to transform *B. subtilis* to Cm^r, generating an insertional mutant via a Campbell type integration (strain PS2465). Southern blot analysis (33) confirmed that all strains had the expected genomic structures (data not shown).

Primer extension. RNA was extracted as previously described from *B. subtilis* PS832 and PS2463 grown in 25 ml of 2× SG medium to an optical density at 600 nm of 2.0 (log phase) (26). Two oligonucleotides, PRA1 (19-mer, 5′CAGCCG

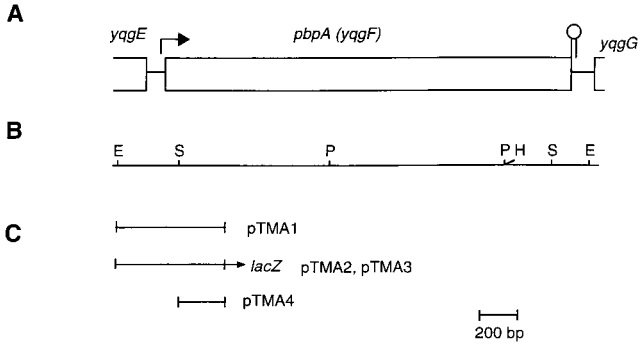

FIG. 1. Map of the *pbpA* (*yqgF*) locus. (A) Open reading frames are indicated by open boxes, and the location and direction of transcription initiation are given by the arrow. A hairpin structure that is likely to be a transcription terminator is shown at the end of the *pbpA* coding region. (B) Endonuclease restriction map of the *pbpA* locus. E, *Eco*RI; S, *Ssp*I; P, *Pst*I; H, *Hinc*II. (C) Plasmid constructs used in the generation of transcriptional *lacZ* fusions (pTMA2 and pTMA3) and the *pbpA* insertional mutant (pTMA4). pTMA1 was used in the construction of pTMA2 and pTMA3.

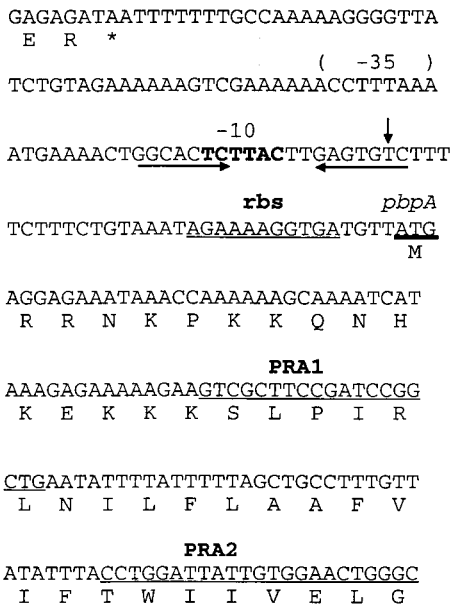

FIG. 2. DNA sequence upstream and including the N-terminal coding region of *pbpA* (bp 135539 to 135807, DDBJ accession no. D84432). The predicted −10 promoter sequence is in boldface, and the transcription start site identified by primer extension is shown by the vertical arrow. An inverted repeat is underlined with arrows. The −35 in parenthesis denotes the region where the −35 recognition sequence would be expected. The underlined ribosome binding site (rbs) is the putative ribosome binding site upstream of the likely translation initiation codon of *pbpA* (thick underline). The amino acid sequences of the C terminus and N terminus of the predicted *yqgE* and *pbpA* open reading frames are shown. The sequences labeled PRA1 and PRA2 are complementary to the two primers used in primer extension analysis to determine the transcription start point of *pbpA*.

GATCGGAAGCGAC3′) and PRA2 (23-mer, 5′GCCCAGTTCCACAATAATCCAGG3′) from within the *pbpA* coding region (Fig. 2) were end labeled with ^{32}P and incubated with 30 to 50 μg of RNA in primer extension reactions as previously described (26). Sequencing of the pTMA1 template was done with the appropriate ^{32}P-labeled oligonucleotide using the chain termination method (31) with the Sequenase kit (U.S. Biochemicals). The primer extension and sequencing reactions were run on a 6% denaturing gel which was dried and exposed to X-ray film with an intensifying screen at −80°C.

Light and electron microscopy of wild-type and *pbpA* outgrowing spores. For light microscopy, 1-ml samples of germinating and outgrowing spores from cultures of strains PS832 and PS2465 were pelleted in a microcentrifuge, resuspended in 1 ml of 0.1% glutaraldehyde in phosphate-buffered saline, pH 7.3 (PBS; 137 mM NaCl, 3 mM KCl, 5.4 mM Na_2HPO_4, 1.7 mM KH_2PO_4) for 30 min at room temperature, and washed with 1 ml of PBS. Fixed germinated spores and cells were photographed by differential interference contrast (DIC) microscopy using a Zeiss confocal laser scanning microscope with a 100× Plan-APOchromat oil immersion lens. Analyses of cell size and volume used Adobe photoshop software with DIC images of cells. Statistical analyses of cell dimensions used Excel 5.0 (Microsoft). For electron microscopy, 5-ml samples of *pbpA* and wild-type outgrowing spores were harvested at various times as described above, prepared, and analyzed as previously described (32).

RESULTS

Identification of *pbpA*. Two different peptides from a tryptic digest of purified PBP2a were partially sequenced giving SVL GSVSSSNEGLPSNLLDHYLSL and GATVLTGLQTGAIN LNTVFKDEPLYI (note that the presence of an internal lysine residue suggests that this peptide was a partial digestion product). These two sequences correspond to amino acids 241 to 264 and 401 to 426 of the predicted protein encoded by a gene identified as *yqgF* (DDBJ accession no. D84432), which maps to about 220° on the *B. subtilis* chromosome. The predicted protein encoded by *yqgF* is 32.7% identical to the *penA* (*pbpB*) gene product, the high-molecular-weight class B PBP2b of *Strep-*

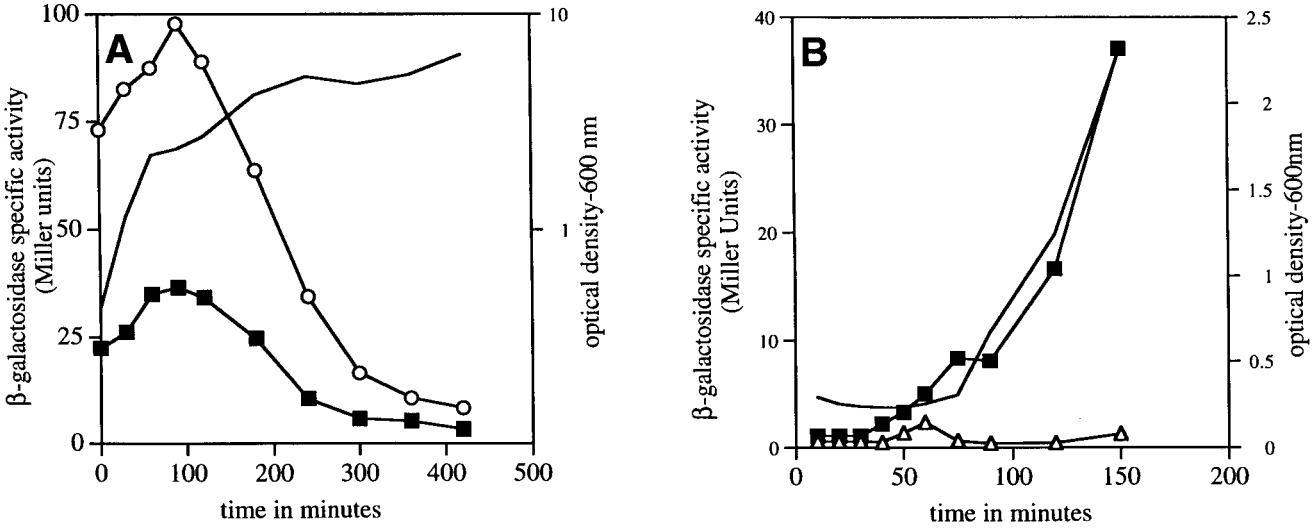

FIG. 3. Expression of *pbpA-lacZ* fusions during growth and sporulation and spore germination and outgrowth. (A) β-Galactosidase specific activity measured from *pbpA-lacZ* fusion strains grown and sporulated at 37°C in 2 × SG medium. (B) β-Galactosidase specific activity measured from germinating *pbpA-lacZ* spores. There was a 35% decrease in the initial optical density early in spore germination, and the lowest attained optical density was used to calculate specific activities during the first 40 min of germination. Symbols: —, optical density; △, wild-type (strain PS832); ■, *pbpA-lacZ* at *pbpA* (strain PS2462); ○, *pbpA-lacZ* at *amyE* (strain PS2463).

tococcus pneumoniae (EMBL accession no. X16022) as determined using tfast software (7) and is 49% similar and 29% identical to PBP2 of *E. coli* (EMBL accession no. X04516), the PBP involved in side wall peptidoglycan synthesis (35). The predicted protein is 716 residues in length (on SDS-PAGE, PBP2a runs at a molecular mass of about 79 kDa) with an amino-terminal hydrophobic sequence consistent with membrane association, as well as the domains conserved in class B PBPs, suggesting that this protein exhibits transpeptidase activity (9, 22). These data strongly suggested that we had identified the gene encoding PBP2a; this was confirmed by insertional mutagenesis (see below). In accordance with nomenclature proposed by Buchanan et al. (5), we have renamed the *yqgF* locus *pbpA*.

Expression of *pbpA*. A fragment encompassing the first 302 bp of the N-terminal coding region and 296 bp upstream of *pbpA* (Fig. 1) was used to generate transcriptional *lacZ* fusions to *pbpA*; these fusions were integrated at both the *pbpA* locus (strain PS2462) and the *amyE* locus (strain PS2463). Analysis of β-galactosidase expression from these constructs demonstrated that levels of *pbpA* transcription appear highest during vegetative growth, with this level dropping continuously after entry into sporulation (Fig. 3A). The rapid fall in *pbpA*-driven β-galactosidase activity as cells enter sporulation must be due at least in part to degradation of β-galactosidase but also suggests that *pbpA* transcription is decreased during this period as well. The pattern of expression of the *pbpA-lacZ* fusion at the *amyE* locus was similar to that of the *pbpA-lacZ* fusion at the *pbpA* locus, indicating that the primary *pbpA* promoter is within the region between *yqgE* and *pbpA*. Surprisingly, expression of the *pbpA-lacZ* fusion at *amyE* was two- to threefold higher than that of the *pbpA-lacZ* fusion at the *pbpA* locus (Fig. 3A). This result was obtained with two different isolates with *pbpA-lacZ* at *amyE*, and Southern blot analysis confirmed that these strains did not have an additional copy of *pbpA-lacZ* at the *pbpA* locus (data not shown). The higher level of expression of *pbpA-lacZ* at *amyE* may be due to the fact that at 25° *amyE* is relatively near the chromosome origin while at 220° *pbpA* is closer to the terminus. Consequently, during vegetative growth there may be more copies of the *amyE* region of the chromosome than of the *pbpA* region.

When spores containing the *pbpA-lacZ* fusion at either *pbpA* or *amyE* were germinated, β-galactosidase activity began to increase after 30 to 40 min and continued to increase thereafter (Fig. 3B and data not shown). This is consistent with *pbpA* being expressed when peptidoglycan must be synthesized for the wall elongation required for spore outgrowth (see below). We also noted a very low but significant level of β-galactosidase in dormant spores of the strain with the *pbpA-lacZ* fusion

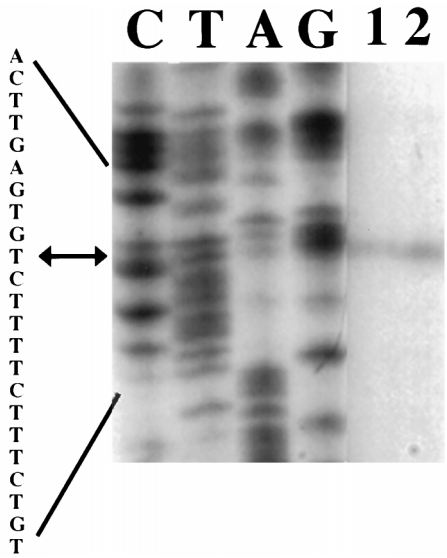

FIG. 4. Primer extension analysis identifying the transcription start point of *pbpA*. RNA was isolated and analyzed as described in Materials and Methods, and primer extension was done with ^{32}P-labeled PRA2 (Fig. 2); the same primer was used to generate the DNA sequencing ladder. The sequence lanes are reversed so that the sequence corresponds to that in Fig. 2. The sequence lanes were visualized after a 48-h exposure of the resulting polyacrylamide gel; primer extension products were visualized after a 2-week exposure. Lane 1, primer extension product obtained using RNA from the wild-type strain (PS832); lane 2, primer extension product obtained using RNA from the strain with a *pbpA-lacZ* fusion at *amyE* (PS2463).

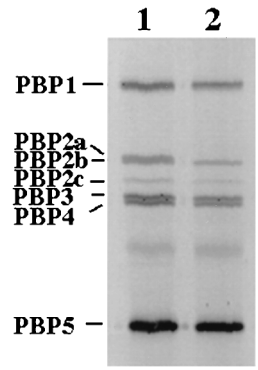

FIG. 5. Analysis of PBPs in the wild-type and *pbpA* mutant strains. Membranes were prepared from 50-ml cultures grown in 2 × SG medium, harvested at an optical density of about 2.0, and incubated with 100 μM FLU-C_6-APA. Approximately 10 μg of total membrane protein was run on an SDS–10% PAGE gel for 4 h at 100 V. The PBPs were visualized with a FluorimagerSI (Vistra) at 500 V and 100 μM scan resolution. The labeled PBPs run in lane 1 and 2 are from the wild type (strain PS832), and the *pbpA* mutant (strain PS2465), respectively. PBPs are numbered as previously described (4, 14).

at the *pbpA* locus (0.5 Miller unit); however, no β-galactosidase activity from *pbpA-lacZ* at the *amyE* locus was observed in dormant spores (<0.1 Miller unit).

Localization of the major *pbpA* promoter. Since analyses of *pbpA-lacZ* fusion expression suggested that the major *pbpA* promoter was between *yqgE* and *pbpA*, we looked for the *pbpA* transcription start site by primer extension analysis using two different oligonucleotides from within the *pbpA* coding region (PRA1 and PRA2, Fig. 2). RNA was extracted from log-phase cells of strain PS832, as well as strain PS2463, to take advantage of the elevated levels of the *pbpA-lacZ* transcript in the latter strain. Using RNA from either strain, analysis of the primer extension product with primer PRA2 revealed a band which initiated at a T residue (denoted +1, Fig. 4) 34 nt upstream of the putative translational initiation codon. Use of PRA1 in primer extension analyses also gave the same transcription start site with each of the RNA preparations (data not shown). Additionally, using either primer, more *pbpA* RNA was present in the strain with the *pbpA-lacZ* fusion at *amyE* (Fig. 4); this was expected given the analyses of *pbpA-lacZ* expression and the presence of a *pbpA* promoter at its own locus as well as at *amyE* in strain PS2463.

The data given above indicate that the *pbpA* transcription start site is identical for both the *pbpA* transcript and the *pbpA-lacZ* transcript at *amyE*. The identification of the promoter within the PCR fragment further indicates that the integration of the *pbpA-lacZ* fusion at *pbpA* does not generate a *pbpA* mutant. Upstream of the identified *pbpA* transcription start site there is a −10 recognition sequence (TCTTAC) which shares three of six residues with the −10 consensus sequence (TATAAT) for RNA polymerase with σ^A (Fig. 2). However, we found no obvious −35 recognition sequence with

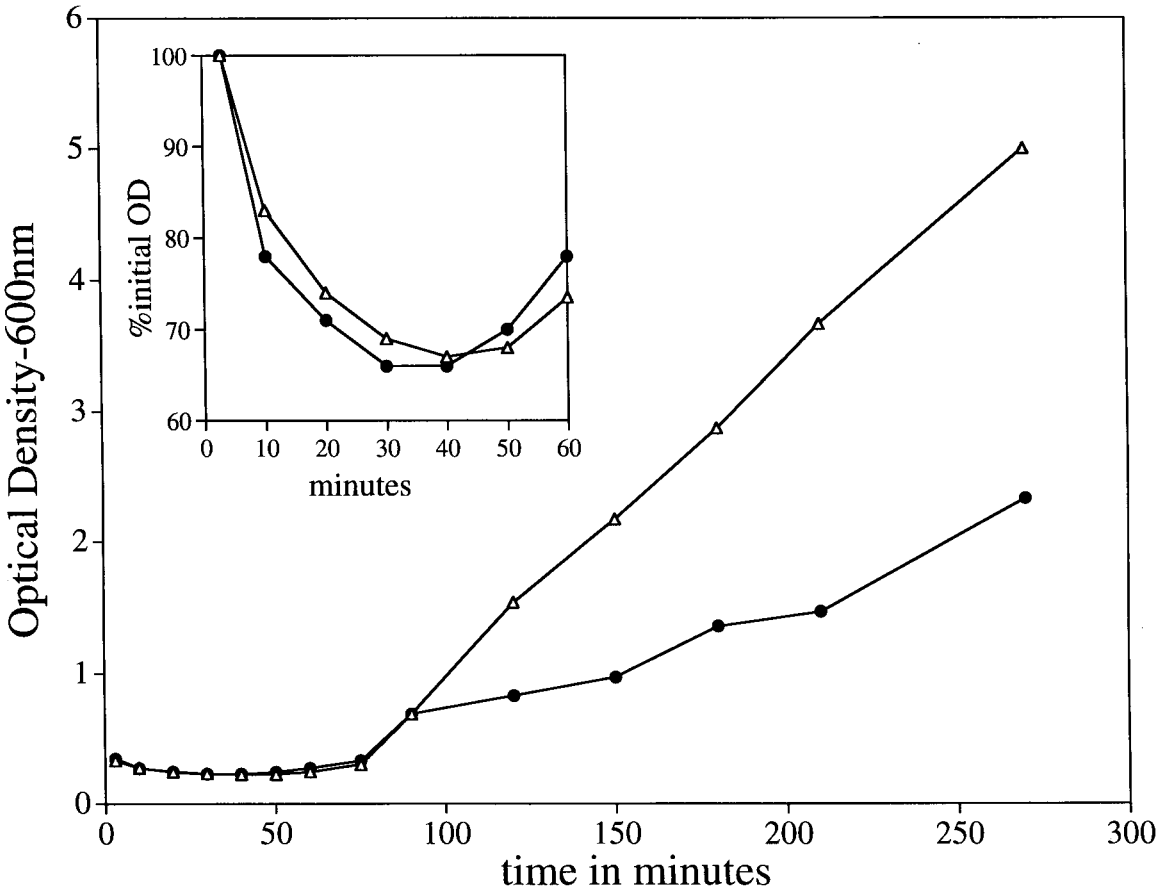

FIG. 6. Germination and outgrowth of wild-type and *pbpA* spores. Spores were heat shocked at 70°C for 30 min and germinated at 37°C in 25 ml of 2× YT medium with 4 mM L-alanine. The initial optical density of each culture was approximately 0.4. The inset shows the optical density as a percentage of the initial value during the first 40 min of germination. Symbols: △, wild type (strain PS832); ●, *pbpA* strain (strain PS2465).

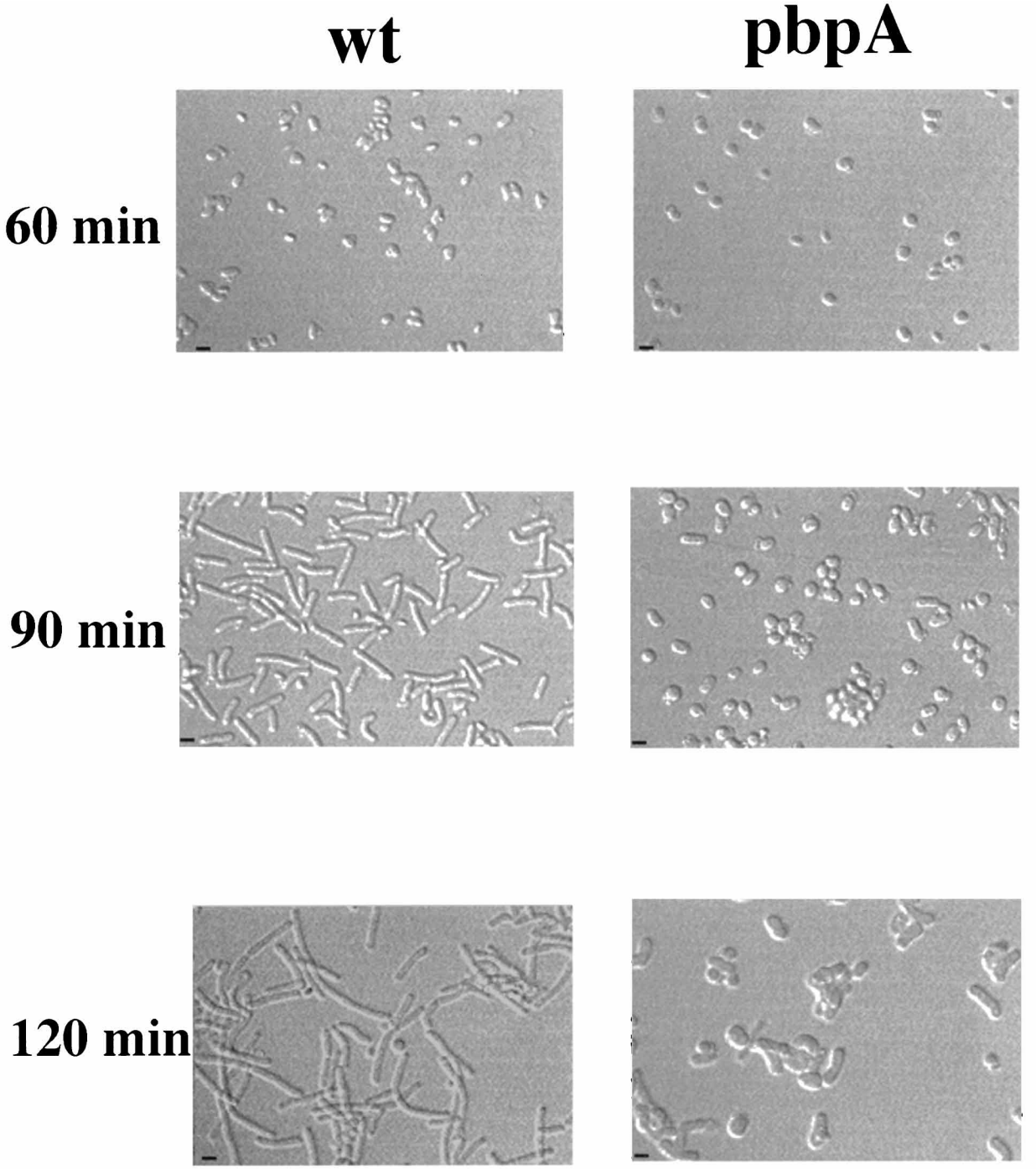

FIG. 7. Light microscopy of outgrowing wild-type and *pbpA* spores. DIC microscopy was used to examine samples from cultures of either *pbpA* (strain PS2465) or wild-type (strain PS832) germinating spores. One-milliliter samples were fixed with 0.1% glutaraldehyde in PBS, placed on a polylysine coverslip, and viewed under a confocal laser scanning microscope with a 100× Plan-APOchromat oil immersion lens. The times on the left are the minutes after the initiation of spore germination. Bars, 2 μm.

reasonable similarity to that recognized by σ^A and with appropriate spacing to the designated −10 sequence in the *pbpA* promoter (Fig. 2). It is of course possible that the transcription start we have assigned by primer extension analysis is actually an mRNA processing site or a site where reverse transcriptase halts in vitro due to template secondary structure. Indeed, there is a potential RNA hairpin just upstream of the transcription start site identified by primer extension which could result in either mRNA processing or the stopping of reverse transcriptase (Fig. 2). Further work may be needed to definitively identify the transcription start site of *pbpA*.

Effects of a *pbpA* mutation. To confirm that *pbpA* encoded PBP2a and to examine the effects of loss of this PBP, an insertional *pbpA* mutant (strain PS2465) was constructed.

Analysis of membranes containing PBPs labeled with FLU-C_6-APA confirmed that strain PS2465 lacked PBP2a and that only PBP2a disappeared in the mutant strain (Fig. 5).

Analysis of the phenotype of strain PS2465 (*pbpA*) compared to that of strain PS832 (wild type) demonstrated no difference in vegetative growth rate in rich media and no morphological differences under light microscopy (data not shown). In addition, the *pbpA* mutant sporulated as efficiently as the wild type, and the *pbpA* spores were fully heat resistant (data not shown). Analysis of purified spore cortex by reverse-phase HPLC following digestion with mutanolysin showed no differences between the wild type and mutant cortices (data not shown). Preliminary HPLC analyses of mutanolysin-digested vegetative cell walls also showed no significant differences between the wild type and *pbpA* mutant strains (data not shown).

The initiation of germination of spores of strains PS832 (wild type) and PS2465 (*pbpA*) was also similar as determined by monitoring the drop in optical density at 600 nm (Fig. 6, inset) and the disappearance of phase-bright spores (data not shown). The *pbpA* and wild-type spores were morphologically similar under both light and electron microscopy after 60 min of germination (Fig. 7 and data not shown), exhibiting similar length-to-diameter ratios (Table 2). However, the *pbpA* mutant spores subsequently exhibited a significant delay in outgrowth as compared to wild-type spores (Fig. 6). Between 60 and 90 min the germinated wild-type spores began to elongate; in contrast, the *pbpA* spores failed to elongate but instead swelled and remained relatively spherical (Fig. 7; Table 2). After 2 h in culture many of the outgrowing *pbpA* spores did begin to elongate although at a significantly larger diameter than the wild-type spores (Fig. 7; Table 2). Interestingly, some of the cells from the outgrowing *pbpA* spores were bent and appeared helical (data not shown and see below), although an increasing number of *pbpA* cells resumed a normal morphology as the optical density of the culture increased (data not shown). Even after 4 h in culture, the majority of the *pbpA* cells directly derived from spores remained larger in diameter than did the wild type (data not shown). However, the calculated average cell volumes of the *pbpA* mutant and the wild type remained comparable throughout germination and outgrowth (Table 2). Comparison of the structures of wild-type and *pbpA* outgrowing spores 2 h after the initiation of germination by electron microscopy confirmed the observations made using light microscopy. The failure to elongate, the increased diameter, and the bent morphology were clearly evident in the *pbpA* mutant (Fig. 8). Additionally, in both wild-type and *pbpA* outgrowing spores, septa were present in most cells by 2 h after the initiation of germination (Fig. 8) and in some cells after 90 min (data not shown).

In order to determine what fraction of *pbpA* spores could resume vegetative growth, equal optical density units of *pbpA* and wild-type spores were plated on LB medium (17) plates. The spores were also counted under the microscope to ensure that there were similar numbers of particles per optical density unit in each spore preparation. This analysis showed that *pbpA* spores formed colonies with about 50% of the efficiency of wild-type spores and that the mutant colonies contained cells which looked morphologically identical to wild-type cells (two separate experiments, data not shown). This suggests that the *pbpA* mutation is not generally lethal to spores, as a substantial number are able to eventually proceed successfully through outgrowth.

TABLE 2. Analysis of dimensions of outgrowing wild-type and *pbpA* spores[a]

Strain	Time (min)	Length (μm)	Diam (μm)	length/diam ratio	Vol (μm^3)
wt[b]	60	2.31 ± 0.37	1.53 ± 0.16	1.51	3.30
pbpA	60	2.15 ± 0.31	1.69 ± 0.24	1.27	3.55
wt	90	5.02 ± 1.11	1.33 ± 0.09	3.77	6.35
pbpA	90	2.51 ± 0.45	1.89 ± 0.27	1.33	5.26
wt	120	7.27 ± 1.74	1.32 ± 0.12	5.51	9.33
pbpA	120	3.79 ± 1.54	2.09 ± 0.37	1.81	10.60

[a] The length and width of 50 outgrowing spores sampled at various times after the initiation of germination were measured from DIC photographs as described in Materials and Methods. Volumes were calculated based on measurements of average cellular length and width assuming the cells were a cylinder with a half sphere on either end. The equation used for this calculation was, as follows: volume = $\pi r^2(l - d) + (4/3)\pi r^3$, where l is length, d is diameter, and r is radius.
[b] wt, wild type.

DISCUSSION

In this study, both peptide sequence analysis of purified PBP2a and insertional mutagenesis of *yqgF* have identified *yqgF* (*pbpA*) as the gene encoding PBP2a. Analysis of the expression of transcriptional *lacZ* fusions to *pbpA* showed that the pattern of *pbpA* expression is consistent with previous reports of PBP2a levels during growth and sporulation (34). Furthermore, *pbpA-lacZ* expression begins to increase 30 to 40 min after the initiation of germination, which is close to the time PBP2a levels were reported to increase (19). It was reported previously that a small amount of PBP2a was present in spores 0 to 15 min after the initiation of germination and that this PBP2a had not been synthesized during germination (19). Consistent with this latter finding, we found a low but significant level of β-galactosidase activity in dormant spores carrying a *pbpA-lacZ* fusion at *pbpA*. Since no β-galactosidase was found in spores carrying *pbpA-lacZ* at *amyE*, the enzyme found in spores containing the *lacZ* fusion at *pbpA* could be the result of read-through from upstream open reading frames encoding putative proteins with sequence similarity to a superoxide dismutase (SOD) (*yqgD*) and a protein commonly associated with SOD (*yqgE*). The presence of SOD activity has recently been demonstrated in spore extracts (6).

Insertional mutagenesis of *pbpA* resulted in loss of PBP2a but had no effect on the phenotype of cells in log phase or sporulation or dormant spores. Although *pbpA* spores initiated germination normally, these spores had difficulty in the transition from a relatively spherical, germinated spore to a cylindrical cell. Electron microscopic analysis confirmed the increase in diameter of *pbpA* outgrowing spores compared to the wild type and demonstrated that septation occurred at about the same time in both wild-type and mutant outgrowing spores. These data suggest that outgrowing *pbpA* spores are capable of synthesizing peptidoglycan but are initially unable to form it into a cylinder. We note that outgrowing *pbpA* spores appear to have a thicker cell wall than do the wild type, but confirmation of this result requires further study. It will clearly be of interest to compare both the rates of synthesis and the structures of peptidoglycan made early in germination and outgrowth of wild-type and *pbpA* spores.

The phenotypic effect of a *pbpA* mutation on spore outgrowth confirms a previous suggestion based on the early synthesis of PBP2a during spore germination and outgrowth and a drop in its expression during stationary phase that PBP2a is involved in the elongation of *B. subtilis* (19). However, it is

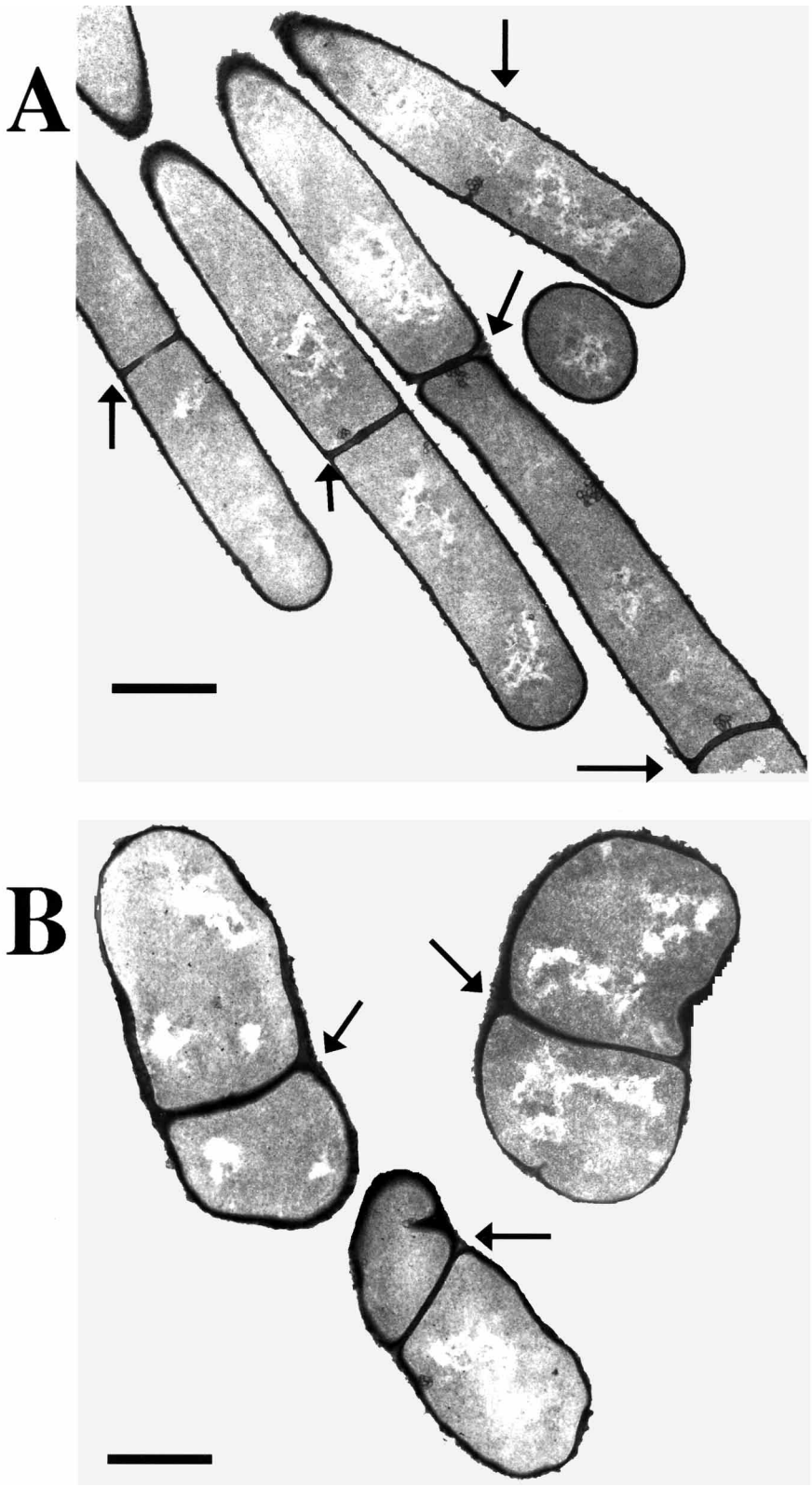

FIG. 8. Electron microscopy of outgrowing wild-type and *pbpA* spores. Outgrowing spores from the wild type, (strain PS832) (A) and *pbpA* strain (strain PS2465) (B) were harvested 2 h after the initiation of germination, fixed, and analyzed by electron microscopy. Septa are indicated by the arrows. The round cell in panel A is in cross section. Bars, 1 μm. Panels A and B are both printed at the same magnification.

important that during vegetative growth, no morphological changes are observed in cells lacking PBP2a. This indicates that PBP2a's role in vegetative elongation is minimal or that other PBPs are able to compensate for PBP2a's contribution to vegetative cell wall elongation in its absence. One explanation for the difference in the requirement for PBP2a in cell growth and spore outgrowth is that other PBPs with compensatory transpeptidase activity are present in sufficient quantities during vegetative growth but are either absent or present in much lower amounts during spore outgrowth. However, many of the *pbpA* cells derived from outgrowing spores eventually attain a normal morphology, possibly as compensatory PBPs are expressed in sufficient levels to suppress the *pbpA* phenotype. It is of course also possible that PBP2a has some special property, such as localization to a specific part of the outgrowing spore's membrane or a unique substrate specificity, which makes it specifically required for efficient spore outgrowth.

We also note that the presence of a low level of PBP2a in the dormant spore suggests that it could be involved in germ cell wall synthesis. This latter structure is thought to serve as the template for the synthesis of the vegetative wall during spore outgrowth (5). If the germ cell wall template is synthesized incorrectly, this could result in problems in proper vegetative wall formation during subsequent spore outgrowth. Again, the role of the peptidoglycan template in determining cell shape during both vegetative growth and spore outgrowth is an important area for further study.

An alternative explanation for the phenotype of the *pbpA* mutant is that problems in cortex degradation could delay outgrowth; however, the presence of a normal cortex structure in the *pbpA* mutant argues against this. While the exact nature of the outgrowth defect in *pbpA* spores remains to be elucidated, we are also interested in trying to determine what events allow an outgrowing *pbpA* spore to eventually form a viable cell. Events to be studied in this regard include more careful study of the timing and placement of the first division septum and the replication and segregation of DNA. As we continue to further characterize the *pbpA* phenotype we will also combine mutations in other PBP-encoding genes with the *pbpA* mutation. By examining the rates of synthesis and the structures of peptidoglycan in these multiple mutants, we may gather further information pertinent to understanding the function of individual PBPs in *B. subtilis.*

ACKNOWLEDGMENTS

This work was supported by grant GM19698 from the National Institutes of Health.

We thank Susan Krueger for assistance with DIC microscopy and Arthur Hand for electron microscopy.

REFERENCES

1. **Anagnostopoulos, C., and J. Spizizen.** 1961. Requirements for transformation in *Bacillus subtilis*. J. Bacteriol. **81:**74–76.
2. **Antoniewski, C., B. Savelli, and P. Stragier.** 1990. The *spoIIJ* gene, which regulates early developmental steps in *Bacillus subtilis*, belongs to a class of environmentally responsive genes. J. Bacteriol. **172:**86–93.
3. **Atrih, A. P. Z., G. Allmaier, and S. Foster.** 1996. Structural analysis of *Bacillus subtilis* 168 endospore peptidoglycan and its role during differentiation. J. Bacteriol. **178:**6173–6183.
4. **Blumberg, P. M., and J. L. Strominger.** 1972. Five penicillin-binding components occur in *Bacillus subtilis* membranes. J. Biol. Chem. **247:**8107–8113.
5. **Buchanan, C. E., A. O. Henriques, and P. J. Piggot.** 1994. Cell wall changes during bacterial endospore formation, p. 167–186. *In* J.-M. Ghuysen and R. Hakenbeck (ed.), Bacterial cell wall. Elsevier Science Publishers, New York, N.Y.
6. **Casillas-Martinez, L., and P. Setlow.** 1996. Unpublished results.
7. **Devereux, H., P. Haeberli, and O. Smithies.** 1984. A comprehensive set of sequence analysis programs for the VAX. Nucleic Acids Res. **12:**387–395.
8. **Ferrari, F. A., A. Nguyen, D. Lang, and J. A. Hoch.** 1983. Construction and properties of an integrable plasmid for *Bacillus subtilis*. J. Bacteriol. **154:** 1513–1515.
9. **Ghuysen, J.-M.** 1991. Serine β-lactamases and penicillin-binding proteins. Annu. Rev. Microbiol. **45:**37–67.
10. **Imae, Y., and J. L. Strominger.** 1976. Relationship between cortex content and properties of *Bacillus sphaericus* spores. J. Bacteriol. **126:**907–913.
11. **Ishino, F., and M. Matsuhashi.** 1982. A mecillinam-sensitive peptidoglycan crosslinking reaction in *Escherichia coli*. Biochem. Biophys. Res. Commun. **109:**689–696.
12. **Ishino, F., and M. Matsuhashi.** 1981. Peptidoglycan synthetic enzyme activities of highly purified penicillin-binding protein 3 in *Escherichia coli*: a septum-forming reaction sequence. Biochem. Biophys. Res. Commun. **101:** 905–911.
13. **Ishino, F., K. Mitsui, S. Tamaki, and M. Matsuhashi.** 1980. Dual enzyme activities of cell wall peptidoglycan synthesis, peptidoglycan transglycosylase and penicillin-sensitive transpeptidase, in purified preparations of *Escherichia coli* penicillin-binding protein 1A. Biochem. Biophys. Res. Commun. **97:**287–293.
14. **Kleppe, G., and J. L. Strominger.** 1979. Studies of the high molecular weight penicillin-binding proteins of *Bacillus subtilis*. J. Biol. Chem. **254:**4856–4862.
15. **Lawrence, P. J., and J. L. Strominger.** 1970. Biosynthesis of the peptidoglycan of bacterial cell walls. The reversible fixation of radioactive penicillin G to the D-alanine carboxypeptidase of *Bacillus subtilis*. J. Biol. Chem. **245:** 3660–3666.
16. **Leighton, T. J., and R. H. Doi.** 1971. The stability of messenger ribonucleic acid during sporulation in *Bacillus subtilis*. J. Biol. Chem. **254:**3189–3195.
17. **Murray, T., D. L. Popham, and P. Setlow.** 1996. Identification and characterization of *pbpC*, the gene encoding *Bacillus subtilis* penicillin-binding protein 3. J. Bacteriol. **178:**6001–6005.
18. **Nakagawa, J., S. Tamaki, and M. Matsuhashi.** 1979. Purified penicillin-binding protein 1Bs from *Escherichia coli* membranes showing activities of both peptidoglycan polymerase and peptidoglycan crosslinking enzyme. Agric. Biol. Chem. **43:**1379–1380.
19. **Neyman, S. L., and C. E. Buchanan.** 1985. Restoration of vegetative penicillin-binding proteins during germination and outgrowth of *Bacillus subtilis* spores: relationship of individual proteins to specific cell cycle events. J. Bacteriol. **161:**164–168.
20. **Nicholson, W. L., and P. Setlow.** 1990. Sporulation, germination, and outgrowth, p. 391–450. *In* C. R. Harwood and S. M. Cutting (ed.), Molecular biological methods for *Bacillus*. John Wiley & Sons Ltd., Chichester, England.
21. **Patel-King, R. S., S. E. Benashski, A. Harrison, and S. M. King.** 1996. Two functional thioredoxins containing redox-sensitive vicinal dithiols from the chlamydomonas outer dynein arm. J. Biol. Chem. **271:**6283–6291.
22. **Piras, G., D. Raze, A. E. Kharroubi, D. Hastir, S. Englebert, J. Coyette, and J.-M. Ghuysen.** 1993. Cloning and sequencing of the low-affinity penicillin-binding protein 3^r-encoding gene of *Enterococcus hirae* S185: modular design and structural organization of the protein. J. Bacteriol. **175:**2844–2852.
23. **Popham, D. L., J. Helin, C. E. Costello, and P. Setlow.** 1996. Analysis of the peptidoglycan structure of *Bacillus subtilis* endospores. J. Bacteriol. **178:** 6451–6458.
24. **Popham, D. L., J. Helin, C. E. Costello, and P. Setlow.** 1997. Muramic lactam in peptidoglycan of *Bacillus subtilis* spores is required for spore outgrowth but not for spore dehydration or heat resistance. Proc. Natl. Acad. Sci. USA **93:**15405–15410.
25. **Popham, D. L., B. Illades-Aguiar, and P. Setlow.** 1995. The *Bacillus subtilis dacB* gene, encoding penicillin-binding protein 5*, is part of a three-gene operon required for proper spore cortex synthesis and spore core dehydration. J. Bacteriol. **177:**4721–4729.
26. **Popham, D. L., and P. Setlow.** 1993. Cloning, nucleotide sequence, and regulation of the *Bacillus subtilis pbpE* operon, which codes for penicillin-binding protein 4* and an apparent amino acid racemase. J. Bacteriol. **175:** 2917–2925.
27. **Popham, D. L., and P. Setlow.** 1993. Cloning, nucleotide sequence, and regulation of the *Bacillus subtilis pbpF* gene, which codes for a putative class A high-molecular-weight penicillin-binding protein. J. Bacteriol. **175:**4870–4876.
28. **Popham, D. L., and P. Setlow.** 1994. Cloning, nucleotide sequence, mutagenesis, and mapping of the *Bacillus subtilis pbpD* gene, which codes for penicillin-binding protein 4. J. Bacteriol. **176:**7197–7205.
29. **Popham, D. L., and P. Setlow.** 1995. Cloning, nucleotide sequence, and mutagenesis of the *Bacillus subtilis ponA* operon, which codes for penicillin-binding protein (PBP) 1 and a PBP-related factor. J. Bacteriol. **177:**326–335.
30. **Popham, D. L., and P. Setlow.** 1996. Phenotypes of *Bacillus subtilis* mutants lacking multiple class A high-molecular weight penicillin-binding proteins. J. Bacteriol. **178:**2079–2085.
31. **Sanger, F., S. Nicklen, and A. R. Coulson.** 1977. DNA sequencing with chain-terminating inhibitors. Proc. Natl. Acad. Sci. USA **74:**5463–5467.
32. **Setlow, B., A. R. Hand, and P. Setlow.** 1991. Synthesis of a *Bacillus subtilis* small, acid-soluble protein in *Escherichia coli* causes cell DNA to assume some characteristics of spore DNA. J. Bacteriol. **173:**1642–1653.

33. **Southern, E. M.** 1975. Detection of specific sequences among DNA fragments separated by gel electrophoresis. J. Mol. Biol. **98:**503–517.
34. **Sowell, M. O., and C. E. Buchanan.** 1983. Changes in penicillin-binding proteins during sporulation of *Bacillus subtilis*. J. Bacteriol. **153:**1331–1337.
35. **Spratt, B. G.** 1975. Distinct penicillin-binding proteins involved in the division, elongation, and shape of *Escherichia coli* K12. Proc. Natl. Acad. Sci. USA **72:**2999–3003.
36. **Sun, D., R. M. Cabrera-Martinez, and P. Setlow.** 1991. Control of transcription of the *Bacillus subtilis spoIIIG* gene, which codes for the forespore-specific transcription factor σ^G. J. Bacteriol. **173:**2977–2984.
37. **Suzuki, H., Y. V. Heijenoort, T. Tamura, J. Mizoguchi, Y. Hirota, and J. V. Heijenoort.** 1980. In vitro peptidoglycan polymerization catalyzed by penicillin binding protein 1b of *Escherichia coli* K-12. FEBS Lett. **110:**245–249.
38. **Todd, J. A., E. J. Bone, and D. J. Ellar.** 1985. The sporulation-specific penicillin-binding protein 5a from *Bacillus subtilis* is a DD-carboxypeptidase *in vitro*. Biochem. J. **230:**825–828.
39. **Warth, A. D., and J. L. Strominger.** 1969. Structure of the peptidoglycan of bacterial spores: occurrence of the lactam of muramic acid. Proc. Natl. Acad. Sci. USA **64:**528–535.
40. **Wu, J.-J., R. Schuch, and P. J. Piggot.** 1992. Characterization of a *Bacillus subtilis* operon that includes genes for an RNA polymerase σ factor and for a putative DD-carboxypeptidase. J. Bacteriol. **174:**4885–4892.
41. **Yanouri, A., R. A. Daniel, J. Errington, and C. E. Buchanan.** 1993. Cloning and sequencing of the cell division gene *pbpB*, which encodes penicillin-binding protein 2B in *Bacillus subtilis*. J. Bacteriol. **175:**7604–7616.